

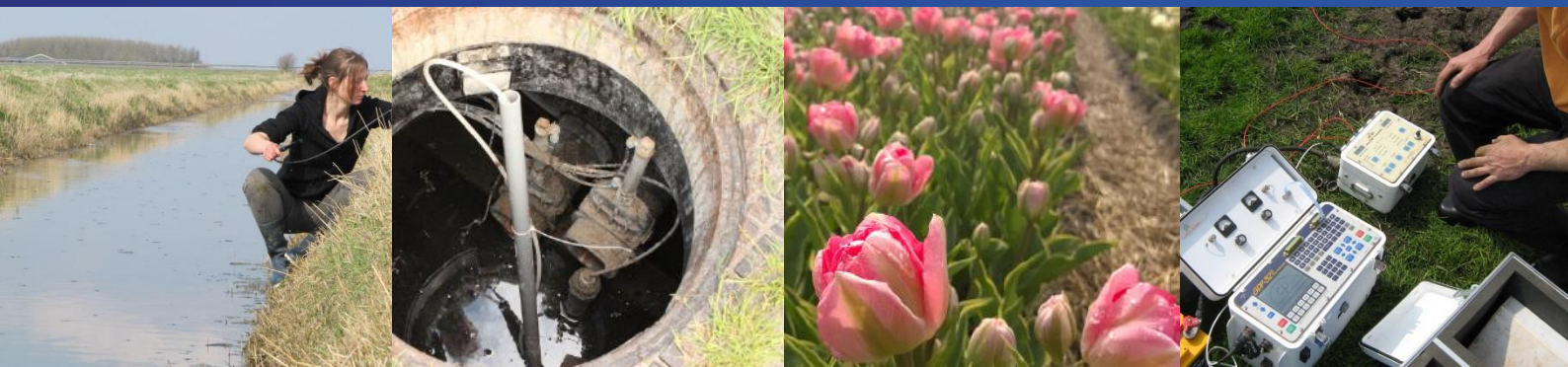
5 March 2018



Literature study

Modelling water flow in a ditches network of a Dutch polder

Roos Godefrooij



Modelling water flow in a ditches network of a Dutch polder

A literature study in preparation of the thesis to obtain the degree of Master
of Science Applied Mathematics at the Delft University of Technology

Roos Godefrooij

5 March 2018

Student number	4487427
Project duration	19 September 2017 until August 2018
Supervisors	Prof. dr. ir. C. Vuik, TU Delft Drs. K. Hu-a-ng, Acacia Water Dr. ir. O. Hoes, Acacia Water



Contents

1	Introduction	5
2	Framework and problem statement	7
3	Hydrological modelling of surface water flow	10
3.1	Flow routing	11
3.1.1	Lumped routing	11
3.1.2	Hydraulic routing	12
3.2	Open channel hydraulics	12
3.2.1	Types of flow	13
3.2.2	Basic definitions and assumptions	14
3.2.3	Energy principles in open channel hydraulics	16
3.2.4	Steady uniform flow	18
3.2.5	Steady nonuniform flow	20
3.2.6	Unsteady flow	20
3.3	The Saint-Venant equations	21
3.3.1	Continuity equation	21
3.3.2	Equation of motion	23
3.4	Geographical features	27
3.4.1	Waterway bifurcations and confluence conditions	27
3.4.2	Weirs	29
3.4.3	Pumping stations, inlets or outlets	30
3.4.4	Culverts	30
3.5	Salinity	30
4	Mathematical problem formulation and solution methods	31
4.1	Flow conservation assuming equilibrium discharge	32
4.2	Flow conservation with backwater effects	35
4.3	Stationary Saint-Venant equations	37
4.4	Kinematic wave model	39
4.5	Diffusive wave model	41
4.6	Dynamic wave model	43

5	Conclusion	45
6	Project proposal	46
6.1	Project goal and research questions	47
6.2	Methods	47
A	Geographical information	54

List of Figures

1	Classification of flows as illustrated in Fig 1-7 of [27]	13
2	Difference in wave lengths around a weir between small and large scales as illustrated in Figure 2.3 and Figure 2.4 in [30]	14
3	Sketch of the crosssectional area of a channel as illustrated in [27]. P is the wetted perimeter, A the cross sectional area and B the channel width.	15
4	The composition of the total energy as illustrated in [27]	17
5	as illustrated and stated in Fig 3 of [32]: "Uniform flow considers the water depth, wetted area and velocity constant at each section through the channel. This means that energy line, water surface and channel bed run parallel."	19
6	Sketch of channel cross sections as illustrated in [27]	21
7	Decomposition of the gravitational force as illustrated in Figure 3.5 in [30]	25
8	Graphical representation of the pressure forces on a control volume as illustrated in Figure 3.7 in [30]	25
9	Network of nodes (grey and white circles and squares) and branches (black arrows), adapted from Figure 1.49 in [34]	29
10	Graphical representation of lumped routing approach with the equilibrium discharge, taken from [30,36]	34
11	Graphical representation of lumped routing approach with the backwater discharge, taken and adapted from [30,36]	37
12	Test problem with two waterway bifurcations	48
13	Map of the ditches network in which the Polder Oude Bildt-pollen is shown in purple on the left of the map. Source: Wetterskip Fryslân [42].	54

List of Symbols

- a Acceleration in m/s^2
- α Coriolis coefficient; a kinetic energy correction coefficient to correct for a nonuniform velocity distribution across a cross sectional area
- α_b Angle of the bottom slope with a given horizontal datum
- B Channel width
- C Chézy coefficient
- c Wave celerity
- d Depth of the water measured from the channel bottom to the water surface
- D Hydraulic depth
- E Specific energy
- g Gravitational constant
- H Total energy
- h Water level or stage; defined as the distance from a given datum to the water surface
- I Outflow in m^3/s
- l_i Length of the i^{th} part of wetted area of the channel related to the wetted perimeter
- L Channel length
- m Mass
- n_m Manning factor
- O Outflow in m^3/s
- P Wetted perimeter
- Q Discharge rate in m^3/s
- Q_l Lateral inflow
- R Hydraulic radius
- ρ Fluid density
- S_0 Channel bed clope
- S_f Slope of the total energy line
- ST Storage function
- τ_0 Bed shear stress
- $\vec{u}(x, y, z)$ Flow velocity field
- p Pressure
- v Average cross sectional velocity
- z_b The distance from given datum to bottom of the channel

1 Introduction

Have you ever visited the Dutch Wadden Sea Region? No, not yet? It is definitely a must visit! Everchanging water channels, seals lying on mud flats and green flat lands with sheep inhabiting the bicycle lanes characterize the area. The Dutch Wadden Sea Region is unique in its kind and its got many things to offer. It has been inscribed on the UNESCO world heritage list since 2009 for its exceptional nature characteristics [1]. The region contains a diverse range of socio-economic activities such as agriculture, fishing, leisure and tourism [2]. Particularly, agriculture has been one of the main determining factors of the coastal, socio-economic and cultural landscape [3]. Think of its small villages, farmhouses, the green fields with ditches and drainage systems; all embodying the classical agricultural wide landscapes. The coastal area is known as one of the best agricultural areas in Europe [4]. More specifically, the west Dutch Wadden Sea coastal region, including the north of North-Holland and West-Friesland, has a large share in the Dutch flower bulb cultivation [4,5]. The northern Dutch Wadden Sea coastal region mainly produces seed potatoes [6,7].

Agriculture in the area relies heavily on water management due to its polder landscape. A polder is a low-lying piece of land enclosed by dikes that is not naturally connected to outside water but of which the hydrological system is manually controlled. Naturally, the area is also susceptible to the effects of climate change, more extreme summer droughts and rising sea levels. Particularly, the Wadden Sea coastal area has a shallow fresh water saline water surface level. Therefore, its agriculture relies on fresh rain water lenses floating on the saline groundwater. It is expected that these fresh water lenses will disappear in the future due to climate change, sea-level rise and land subsidence [4]. Hence the increasing water salinity results in salinization of the available water which can become damaging to the crops and their agricultural yield [8]. So how do we deal with salinization and how do we ensure the availability of clean fresh water?

There are different possible approaches to this challenge; namely, desali-

nating sea water, switching to salt minning agriculture, selective breeding of crops to increase their salt and drought tolerance or implementing measures to reduce fresh water losses and use the available fresh water as efficiently as possible [9]. Desalinating sea water might sound as the perfect solution, however, it is still a very energy consuming and therefore expensive process which produces a large amount of greenhouse gases [10, 11]. Making the switch to cultivating alternative salt minning crops is currently not economically feasible for many farmers due to low market demands of the alternative crops. On the other hand, selective breeding and improving drought and salt tolerance levels of the current crops is seen by the farmers as an option worth exploring further [12]. Improving the salt tolerance of current crops is being researched at Salt Farm Texel by numerous research institutes such as VU University, Wageningen University and Research, the Wadden Academy, and more. The project started in 2006 and has continued ever since with the aim to investigate the opportunities of saline agriculture and hence serve as an example for the other coastal agricultural areas in the Netherlands [13, 14]. Finally, a straightforward approach is to investigate the exact processes underlying fresh water losses and to subsequently find measures to reduce these losses. Important to note is that the effects of climate change on the salinization of Dutch agricultural areas is a relatively new research area. Knowledge on the effects of salinization on local levels is missing. Accordingly, more research is needed to predict future effects of climate change, sea-level rise and subsidence on the ground and surface water [12, 15].

For this reason, Acacia Water and the Waddenfonds started the project Spaarwater in 2013 to investigate mitigation measures for increasing salinization. Its main aim is to safeguard and improve fresh water supplies, whilst taking the mitigation measures' technical and economic feasibility into account. Therefore, an additional focus is on reduction of plants diseases (such as Brown Rot) and on drainage of pesticides and unwanted nutrients. Accordingly, an important result is the protection and increase of the crops' yields. The project is carried out in cooperation with multiple organizations such as provincial water authorities, provincial governments, agrarians and

agricultural business organizations in the Dutch coastal Wadden Sea region. Altogether, there are four pilot locations in the Provinces of Noord-Holland, Friesland and Groningen [4].

The water ditches in the farmlands are part of a complex hydrological system. Therefore, it is labour intensive to check the effects of each of the mitigation measures on the land's salinization locally. Hence, there's the ambition to develop a web application with underlying mathematical tools to predict the local effects of introducing a mitigation measure. In this literature review, we will investigate how to best design such a tool and particularly what mathematical algorithms can be used for it to work fast . We will first introduce some important hydrological concepts. Subsequently, we will elaborate on the problem statement, my research strategy and the scope of this study. Then we will continue with giving an overview of the hydrological concepts behind modelling open channel water flow and we will zoom into examples of existing hydrological models. Followingly, we will research the main mathematical theory behind modelling this problem and investigate how to apply the theory effectively. We will finish with concluding remarks and with a project proposal for the continuation of the research.

2 Framework and problem statement

The above-mentioned salinizing farmlands in the Dutch polders are the focus of this research. For clarification, in this study we talk of salinization in an agricultural area if the water is too salty for optimal land use, or equivalently, if it has an excessively high chloride content which is limiting optimal land use [16, 17]. For now we do not specify salinization by a number because harmful chloride concentrations highly depend on the type of crop.

Historically, research into salinization of agricultural land in the Netherlands has mostly been related to the effects of extreme floods. However, there has always been a more gradual, continuing process of salinization as well; namely, salinization of surface water because of sea water entering through coastal inlets and salinization of ground water through saline seepage. Saline

seepage is a process that occurs in coastal areas that lie below mean sea level. Saline groundwater is pushed upward to the surface due to the hydrostatic pressure difference with the surrounding more elevated areas [12, 18]. Specifically in the Netherlands, a country well known for its land reclamations and low lying polders, seepage is an ever occurring process.

Salt accumulates in the soil during summer time especially, due to the combination of seepage and evaporation. The net rain fall during the winter months has in the Netherlands generally been sufficient to wash out the in summertime accumulated salt to the sea. Flushing the ditches is normally done with excess rainwater diverted from the rivers Rhine and Meuse and the lake IJsselmeer [12, 19]. However, it is expected that climate change will give rise to longer and more intense drought intervals resulting in smaller rainwater lenses and diminishing freshwater supplies from the Rhine, Meuse and the IJsselmeer. In addition, sea-level rise and land subsidence increase hydrostatic pressure differences and accordingly intensify seepage [12, 18, 20]. Agriculture in the Wadden Sea coastal region of the Netherlands is possible because of fresh rainwater lenses floating on the saline water. Saline water is pushed upwards but will stay below the fresh water lenses due to its higher density. There's a mixed groundwater zone between the saline seepage and the freshwater lenses, in which chloride concentrations increase with depth. Accordingly, the rainwater lenses ensure fresh water supply in the crops' root zones. When the fresh water lenses become thinner in dry periods, saline water reaches the root zone which can be harmful for agricultural yields [8, 21, 22]. In summary, reasonable worries exist that dryer summers and diminishing water supplies for flushing the ditches will result in salinization and even irrigation water shortages.

Hence, Acacia Water is researching several mitigation measures for the increasing salinization and freshwater shortages. The main mitigation measures researched in the Spaarwater project are as follows [4];

1. Establishing locally self-sufficient water supplies by either artificially managing groundwater recharge or by creating underground fresh water buffers

2. Enlarging the freshwater lenses through reducing salinization by system specific drainage
3. Implementing new irrigation methods, such as drip-irrigation, to use the available freshwater as efficiently as possible

Acacia Water tests the effects of these mitigation measures by determining the salinity of water with an electrical conductivity (EC) meter. Electrical conductivity easily translates to salt content. Therefore, an EC meter is a simple and quick tool for determining salinity levels. A great advantage is that farmers can also do these measurements themselves with a simple device connected to their mobile phone. Accordingly, they collect datapoints about the water's salinity over time. Hence, Acacia Water would like to use this data to develop a better understanding of the water system and salinization in a polder's ditches network. The first idea was to simply connect the datapoints by interpolating the data. For interpolating the data, one needs to know about the water flow in the infrastructure of a ditches network. More specifically, one needs to know about the governing mathematical laws of the water flow.

The aim of this literature review is to investigate existing hydrological models, and their underlying mathematical theory, suitable for modelling the water flow in a ditches network in the coastal Wadden Sea region. In addition, we will investigate general mathematical theory and algorithms applicable for this case. This is a preparatory study for the follow-up practical research project of designing and implementing such a model. Ultimately, the model should give a general overview of the effects of a mitigation measure on the water flow, water salinity and sediment transport.

Important for the first design of a model is that it is simple and runs fast whilst keeping in mind that complexities can be added later. Therefore, in this study we will solely focus on modelling water flow in a ditches network. We will start with a simple network with one inlet and one outlet. Subsequently, we will increase complexity by adding geographical features one by one. Think for example of waterway junctions, dams, culverts and dead-end drains. Our final ambition is to apply the model to a ditches network of a real life polder;

namely, the Oude Bildtpollenpolder, located in North Friesland. Note that the addition of water salinity to the model, in the form of chloride ion transport, is the next step in the model development. Hence, this will be kept in mind throughout the process of development of the water flow model.

Students of the VU university and Wageningen University and Research (WUR) have previously looked into salinization of the Dutch polders in North Friesland. Two studies have been done in 2016 on the effects on water salinity of flushing the ditches [23,24]. Another study was done by four WUR students and focused on the effects of climate change on the Dutch polders [21]. They have modelled the water and salt fluxes between the ground water and the surface water in the Oude Bildtpollenpolder. We will use the concepts used in these studies and take the outcomes of the models into account for design of the surface water model. The latest study was done by WUR student Luc Scholten. He has automatized the digitalisation of the infrastructure of the waterways of a polder such that a mathematical model can be applied to it. More specifically, he automatized the discretisation of the waterways which means that the data of the waterways are cut into bitesize chunks that can be used as input for interpolation. In addition, he made a start with researching possible algorithms for mathematical modelling of the surface water flow using the Oude Bildtpollen polder as a case study [25]. We will use his findings as a starting point. In particular, the automatized discretization of the waterways can be used in our modelling of the real life scenario.

3 Hydrological modelling of surface water flow

A variety of different hydrological transport models were developed since the increase in the computer's computational power and the rising demands for detailed numerical forecasting. Hydrological transport models simulate stream flow and calculate water quality parameters, with varying modelling purposes; for example, groundwater transport, surface water flow, sediment transport and so forth. We focus on surface water modelling in this study, and more specifically, on open channel flow. Open channel flow entails the study of

water flow with a free surface, which is subject to atmospheric pressure and is driven by gravity [26, 27]. Ultimately, we want to learn about the amounts of water that flow past a specific point in a ditch over time. It is a first necessary step for eventually getting an idea of the saline and fresh water flows.

Hydrological models can be broadly categorised into *stochastic* and *deterministic* models. In a *stochastic* model, a given input generates output with a random component; whereas in a *deterministic* model, a given input always generates the same output. We will only consider deterministic models in this study. Deterministic models can, in its turn, be categorised into *lumped* and *distributed* models. In a deterministic lumped model, the system is averaged over a given distance in space, hence not considering the hydrological processes taking place in between the startpoint and endpoint of this distance. On the other hand, a deterministic distributed model considers the hydrological processes taking place at multiple points of this given distance and defines the model variables as functions of space [28].

3.1 Flow routing

In hydrology, modelling surface water flow is generally done through flow routing. It is a commonly used technique to determine changes in the waterflow rates at multiple points of a channel from known or assumed hydrographs. A hydrograph is a graph showing the rate of flow (discharge) as a function of time at a given location on the channel [28]. Flow routing is used in flood forecasting for example. Routing makes use of the continuity principle resulting from the assumption that the given system is closed; which means that the total amounts of inflow and outflow are equal and that there is no external inflow. Routing methods are broadly separated into two classes; namely, hydrologic (lumped) routing and hydraulic (distributed) routing.

3.1.1 Lumped routing

In lumped routing, the channel is divided into multiple boxes which each represents one reach (one length of the river). Here, inflow and outflow are linked by simple equations not associated with specific hydrological processes.

Flow rates between boxes are set by parameters which have to be determined empirically and optimized by comparing the observed and the computed data [29]. Mathematically, inflow $I(t)$, outflow $O(t)$ and storage $ST(t)$ are related by the continuity equation given in [26, 28]:

$$\frac{dST}{dt} = I(t) - O(t) \quad (1)$$

Note that in order to solve this system mathematically, a second relationship is needed to relate ST with I and O . In general, this is referred to as the storage function ST and may be written as an arbitrary function of I , O and their time derivatives [28]:

$$ST = f\left(I, \frac{dI}{dt}, \frac{d^2I}{dt^2}, \dots, O, \frac{dO}{dt}, \frac{d^2O}{dt^2}\right) \quad (2)$$

3.1.2 Hydraulic routing

In contrast, hydraulic routing determines the waterflow as a function of both space and time. This is done by solving the governing (partial differential) equations of unsteady open channel flow, called the Saint-Venant equations. These will be discussed more elaborately in a later section. Here, unsteady refers to an instationary process in which water flow velocity varies with time. Hydraulic routing requires a detailed geographical and hydrological description of the research area in order to solve the partial differential equations [26, 29].

3.2 Open channel hydraulics

Whereas routing is a specific type of modelling open channel flow using hydrographs, the study of open channel hydraulics refers to a more general research area which is concerned with modelling water flow using the Saint-Venant equations. In the following paragraphs, we will first discuss the different types of open channel flow, second we will introduce basic definitions and assumptions, third we will discuss their underlying energy principles and followingly we will outline the governing equations of the different open channel flow types.

3.2.1 Types of flow

Open channel flow is categorized according to steadiness, a condition related to time, and uniformity, a condition related to space. In *steady* open channel flow, the water flow velocity at any point of observation does not change with time, hence it is a stationary process; whereas flow is *unsteady* when the water flow velocity at a specific point changes from moment to moment, which is an instationary process. Open channel flow is *uniform* if flow velocity is constant at all points along the channel at all times; whereas flow in *nonuniform*, also called varied, if the flow velocity changes with water moving along the channel. Varied flow is usually subcategorized into gradually varied flow and rapidly varied flow, where the flow varies gradually if the flow velocity varies slowly with respect to distance and the flow varies rapidly if the flow velocity varies significantly over a short distance [26, 27]. More specifically, rapidly varied flow refers to a situation in which changes in depth and velocity occur over short lengths; considering a scale of a maximum of a couple of meters. Think of flows beneath sluice gates or over weirs. Gradually varied flow refers to a situation in which flow changes in depth and velocity occur over long distances; considering a scale of tens of kilometers [30]. In this study we focus on the latter; namely, gradually varied flow. We are merely interested in the water flow over the entirety of a ditches network of about 10 kilometers in length. Hence, we will neglect the short and local waves occurring around weirs and sluice gates. The classification of open channel flow is shown in Figure 1 and a graphical representation of the difference between gradually and rapidly varied flow is shown in Figure 2.

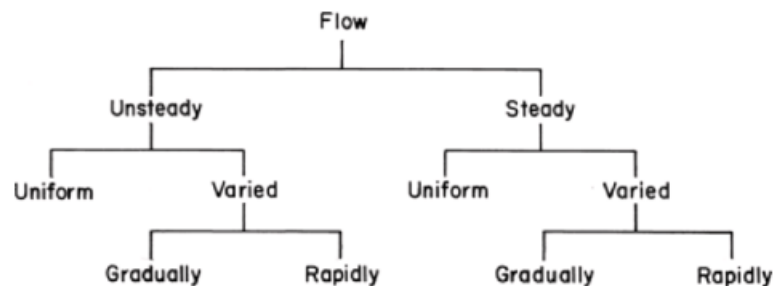


Figure 1: Classification of flows as illustrated in Fig 1-7 of [27]

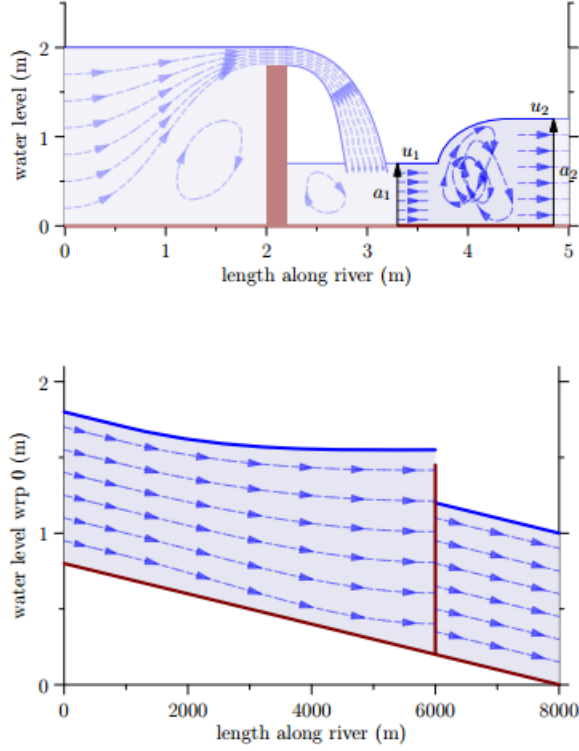


Figure 2: Difference in wave lengths around a weir between small and large scales as illustrated in Figure 2.3 and Figure 2.4 in [30]

3.2.2 Basic definitions and assumptions

The description of open water waves in channels is given by :

The flow velocity field $\vec{u}(t, x, y, z)$

The pressures $p(t, x, y, z)$

The water depths $d(t, x, y)$

which results in a complex system with three variables varying in three or four dimensions. Hence, these dependencies need to be partly relaxed and simplified to enable open water flow calculations [30]. In this section we shall introduce basic definitions and discuss the assumptions commonly made to simplify the open water flow equations to describe the waves as one dimensional in space.

For every position x along a channel, the *cross section* A is the unique plane perpendicular to the flow direction along the channel. We will assume a horizontal water level in each cross section and the geometry of each cross section to be completely known. Moreover, $z_b(x)$ denotes the lowest point of

the cross section at x . The lowest point z_b is measured from an arbitrary horizontal zero fixed for the whole channel and usually taken to be sea level.

The *wetted perimeter* P is defined as the cross sectional area of the channel that touches the water, as is also illustrated in Figure 3. Mathematically, the wetted perimeter can be defined by

$$P = \sum_{i=0}^{\infty} l_i \quad (3)$$

where l_i is the length of each surface in contact with the water. Followingly, the *hydraulic radius* R and the *hydraulic depth* D are defined by

$$R = \frac{A}{P}$$

$$D = \frac{A}{B}$$

with A being the cross sectional area and B the channel width.

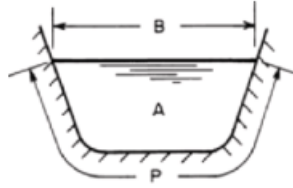


Figure 3: Sketch of the crosssectional area of a channel as illustrated in [27]. P is the wetted perimeter, A the cross sectional area and B the channel width.

The amount of water flowing through a particular cross section, at a given time, is determined by the velocity field $\vec{u}(t, x, y, z)$. Since we are focusing on large wavelengths and large scales, we are merely interested in the average velocity and total water flow in a cross section. To quantify this, we define the *discharge* Q as the volumetric flow rate of water through a given cross sectional area A (hence with a dimension of m^3/s). Mathematically, the discharge is given by

$$Q(t, x) = \int \int_{(y,z) \in A} u_x(t, x, y, z)$$

which simplifies to

$$Q(t, x) = A(t, x)v(t, x) \quad (4)$$

where $v(t, x)$ is the *average velocity*, over a given cross section $A(t, x)$, given by

$$v(t, x) = \frac{1}{A(t, x)} \int \int_{(y,z) \in A} u_x(t, x, y, z)$$

[30].

Another important simplifying assumption is that of *hydrostatic pressure*, i.e. the pressure behaves the same as in still water. Again, we may make this assumption because of the long waves. Hydrostatic pressure means that at every point in the river, the pressure equals the static pressure of the water column above. Hence, the pressure increases linearly from the top to the bottom of the channel [30]. The relationship between pressure p and height z is given by

$$p(t, x, z) = \rho g(d(t, x) - z) \quad (5)$$

where ρ is the volumetric mass density, g is the gravitational constant, $d(t, x)$ is the depth and z is the height of the point of consideration measured from the lowest bottom point z_b . Hence, the pressures for all the points in each cross section along the channel are known. Thus the pressure p is considered to be a given quantity.

3.2.3 Energy principles in open channel hydraulics

Before we dive into the specifics regarding the different types of open channel flow, we will shortly introduce the energy principles needed for deriving the equations for steady uniform and steady nonuniform flow. The total energy at any point of an open channel is the sum of the elevation energy, pressure energy and kinetic energy; where the elevation and pressure energy together form the potential energy. The elevation energy refers to the elevation of the channel bed above a specified datum. In open channel flow, there is atmospheric pressure at the free surface. Therefore, the pressure is relatively constant and the water surface is taken as the pressure reference for convenience [31].

At a given cross section in an open channel, the specific energy E is defined as the energy per unit weight of water, with the channel bottom used as a datum. H is the total energy, which is the total energy per unit weight of

water measured from a horizontal datum, for example the mean sea level. Hence, the specific energy E and the total energy H at a given cross section are not generally equal. For a fixed point x along the channel, the specific energy E is given by

$$E = d + \alpha \frac{v^2}{2g} \quad (6)$$

where d is the water depth, the term $\frac{v^2}{2g}$ is the kinetic energy term in which v is the average cross sectional velocity and α is the velocity coefficient used to account for nonuniformity in the velocity distribution when taking the average velocity over the cross sectional area at point x . When assuming a uniform velocity distribution, α can be set to equal $\alpha = 1$. The total energy H is given by

$$H = z_b + d + \alpha \frac{v^2}{2g} = z_b + E \quad (7)$$

where z_b is the distance from the specified horizontal datum to the channel bed. Figure 4 shows the composition of the total energy at a given cross section. It also shows the energy grade line, which is given by the total energy H along all points x along the channel. S_f is known as the slope of the total energy line and is evaluated by

$$S_f = \frac{dH}{dx} = \frac{dz_b}{dx} + \frac{dE}{dx} \quad (8)$$

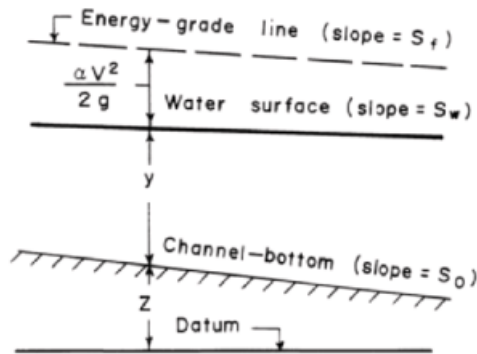


Figure 4: The composition of the total energy as illustrated in [27]

3.2.4 Steady uniform flow

Steady flow represents a stationary process, which is solely a function varying in space and not in time. Thus, for steady flows the time derivative equals zero:

$$\frac{dv}{dt} = 0$$

In open channel hydraulics, one usually first considers the stationary process in order to get a general idea of the direction of flow, the variation in flow rate and flow depth along a channel. More specifically, here we start with considering steady uniform flow in which also the spatial derivative equals zero:

$$\frac{dv}{dx} = 0$$

Hence, uniform flow in a channel represents a state of dynamic equilibrium. It occurs when the depth of the water, the wetted channel surface area (wetted perimeter) and the flow velocity remain constant in both time and in space, along the channel. Naturally, open channel flow is governed by gravity. The water flow in encounters resistance as it flows down the sloped channel bottom. In a dynamic equilibrium, the gravitational force causing the downflow is equal and opposite to the resistance forces obstructing the flow [31, 32].

Equations describing the relation between friction and flow velocity for steady uniform open channel flow have been developed semi-empirically, based on field measurements and scale models [32]. Those formulas relate velocity of flow to the hydraulic radius, R , and slope of the channel bed, S_0 . Chézy was the first who developed such an equation, given by

$$v = C\sqrt{RS_0} \tag{9}$$

where

v is the average velocity of the water flow (ms^{-1})

C is Chezy's coefficient of boundary roughness ($m^{\frac{1}{2}}s^{-1}$)

R is the hydraulic radius (m) which is defined by $\frac{A}{P}$; wetted area, A , divided by wetted perimeter, P

S_0 is the channel bed slope or hydraulic gradient (dimensionless)

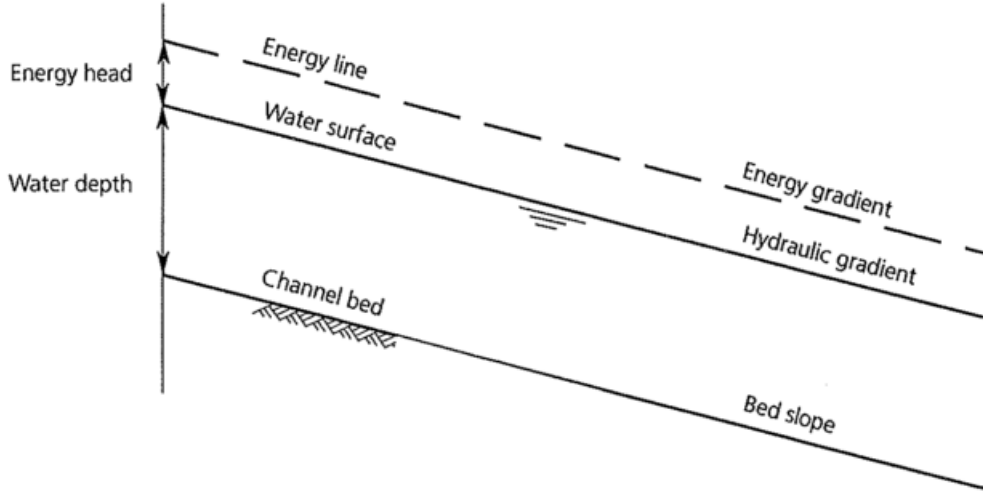


Figure 5: as illustrated and stated in Fig 3 of [32]: "Uniform flow considers the water depth, wetted area and velocity constant at each section through the channel. This means that energy line, water surface and channel bed run parallel."

Chézy proposed his Equation(9) in 1775 for the design of water supply channel near Paris. His work was not published until 1897 and only became widely known after that year [26]. The Chézy coefficient of boundary roughness has to be determined empirically.

Around that time, the Irish engineer Robert Manning carried out an empirical research investigating the relation between the average velocity, hydraulic radius and channel bed slope. This resulted in the Manning equation, which he published in 1889, being

$$v = \frac{1}{n_m} R^{\frac{2}{3}} S_0^{\frac{1}{2}} \quad (10)$$

where the Chézy coefficient in equation (9) is replaced by $C = \frac{1}{n_m} R^{\frac{1}{6}}$. The n_m in Manning's Equation (10) is referred to as the Manning factor n_m , a factor relating the resistance to the roughness of the channel boundaries. Again, Manning's n_m is to be determined empirically. Various studies have been done to provide guidance in choosing appropriate values for n_m . It is common practice to assume that the Manning factor n_m is not a function of depth, hence a constant value n_m is considered for a given channel reach [31]. To

summarise, the above-mentioned Chézy and Manning equations have been widely in use for estimating the average flow velocity for steady uniform flow in open channels. It depends on tradition or convenience which formula of these two will be chosen [32]. In order to do so, the roughness constants have to be estimated empirically for a given channel which could in itself be a separate research study.

3.2.5 Steady nonuniform flow

Similarly, Chézy's and Manning's equations hold for steady nonuniform flow. The only difference being the slope term; namely, S_f is considered instead of S_0 . S_f is known as the slope of the total energy line (dH/dx) as is given in Equation (8). In uniform flow the energy gradient equals the channel bed slope. However, this is not the case in nonuniform flow since the flow velocity changes along the channel [27, 31]. Accordingly, Chézy's equation becomes

$$v = C\sqrt{RS_f} \quad (11)$$

and Manning's equation becomes

$$v = \frac{1}{n_m} R^{\frac{2}{3}} S_f^{\frac{1}{2}} \quad (12)$$

which can also be rewritten, using $A = Qv$, as

$$S_f = \frac{n^2 Q |Q|}{A^2 R^{2/3}} \quad (13)$$

3.2.6 Unsteady flow

In unsteady open channel flow, flow velocities and depths change with time at any fixed spatial position in the channel. Naturally, open channel flow in channels is unsteady and nonuniform because of the free surface. Mathematically, this means that the two dependent flow variables, velocity and depth, are functions of both distance x along the channel and time t . Hence, mathematical problem formulation requires two partial differential equations representing the continuity and momentum principles in the two unknown de-

pendent variables [26]. These equations are called the Saint-Venant equations or the dynamic wave equations. They have been derived from the more general Navier-Stokes equations describing the motion of viscous fluid substances. Analytical solutions to the the Saint-Venant equations can only be found in extremely simplified forms. Hence, this led to the development of numerical techniques to approximate solutions for the governing equations [26]. The Saint-Venant equations and the available solution techniques will be discussed in the following sections.

3.3 The Saint-Venant equations

The Saint-Venant equations consist of two partial differential equations describing the continuity and momentum principles. We derive the Saint-Venant equations by considering a control volume of a channel, which is an infinitesimal part of the river between the cross sections at x and at $x + \Delta x$. Accordingly, we calculate the mass and the momentum that flows through the control volume. In addition, we calculate the change in storage between times t and $t + \Delta t$.

3.3.1 Continuity equation

The continuity equation is based on the conservation of mass principle. Let us first consider an open channel with no lateral inflow, meaning that there is no water flowing in from the sides of the river or from a reservoir. In this channel, consider a control volume with two cross sections 1 and 2, as illustrated in Figure 6.

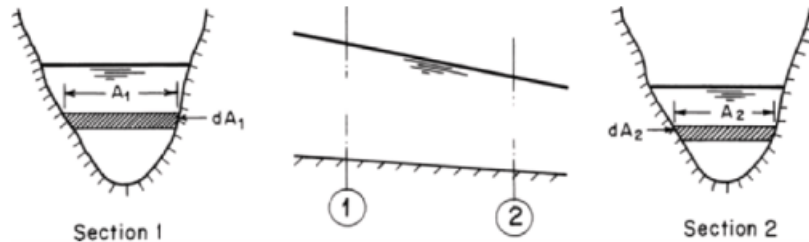


Figure 6: Sketch of channel cross sections as illustrated in [27]

For this volume it must hold that in a specific time interval Δt , the inflow

volume equals the outflow volume. Usually, this principle is expressed in discharge Q which is the volumetric flow rate of water that is transported through a given cross sectional area [33]. Simply said, the cross sectional area in section 1 is larger than in section 2. Therefore, the volumetric flow rate is smaller at point 1 than at point 2.

Incorporating lateral inflow gives that the change in storage equals the sum of the lateral flow with the difference between inflow and outflow. Followingly, we will discuss each of these terms to eventually arrive at the continuity equation.

The *change in storage* is the change in mass in the control volume from time t to time $t + \Delta t$. With $\rho A(t, x)\Delta x$ being the mass in the control volume at time t , we get

$$\begin{aligned} \text{change in storage} &= \Delta x(\rho A(t + dt, x) - \rho A(t, x)) \\ &\approx \frac{\partial \rho A}{\partial t}(t, x)\Delta x\Delta t \end{aligned}$$

The *difference between inflow and outflow* relates to the discharge $Q(t, x)$. At x , the discharge flowing into the control volume is $Q(t, x)$. Hence, the total amount of water entering the control volume between times t and $t + \Delta t$ equals $\Delta t\rho Q(t, x)$. Over the control volume we get

$$\begin{aligned} \text{flow in - flow out} &= \Delta t(\rho Q(t, x) - \rho Q(t, x + \Delta x)) \\ &\approx -\frac{\partial \rho Q(t, x)}{\partial x}\Delta x\Delta t \end{aligned}$$

The *lateral flow* $Q_l(t, x)$ refers to the inflow or outflow of water outside of the river due events such as rainfall, seepage or evaporation. The total lateral flow into the control volume is specified by

$$\rho Q_l(t, x)\Delta x\Delta t$$

where $Q_l(t, x)$ can be taken as a constant or as a function of time and/or space.

Finally, this leads to the continuity equation given by

$$\begin{aligned} \text{change in storage} &= \text{inflow} - \text{outflow} + \text{lateral flow} \\ \frac{\partial \rho A}{\partial t}(t, x) \Delta x \Delta t &= -\frac{\partial \rho Q(t, x)}{\partial x} \Delta x \Delta t + \rho Q_l(t, x) \Delta x \Delta t \end{aligned}$$

which can be simplified, by taking $\rho = 1$ constant for the density of water, to

$$\frac{\partial A}{\partial t}(t, x) = -\frac{\partial Q(t, x)}{\partial x} + Q_l(t, x)$$

hence resulting in the continuity equation

$$\frac{\partial Q}{\partial x} + \frac{\partial A}{\partial t} = Q_l \quad (14)$$

3.3.2 Equation of motion

For deriving the equation of motion, we consider conservation of momentum in x direction which is the direction of flow. Momentum is defined by mass times velocity; mv . Hence, the change in momentum is defined by

$$\frac{\partial mv}{\partial t} = m \frac{\partial v}{\partial t} = ma = F$$

where a is the acceleration and F the sum of the external forces in the x direction. In a similar manner as was discussed in the previous section, the mass in the control volume is defined as $\rho A(t, x) \Delta x$. Hence, the momentum is given by $\rho A(t, x) v(t, x) = \rho Q(t, x)$ which gives a change in storage of momentum given by

$$\text{change in storage of momentum} = \rho \frac{\partial Q(t, x)}{\partial t}$$

In addition, the total amount of momentum in the control volume between t and $t + \Delta t$ equals $\Delta t Q(t, x)v(t, x)$. Thus, we get

$$\begin{aligned} \text{momentum inflow} - \text{momentum outflow} &= \\ &= \Delta t[\rho Q(t, x)v(t, x) - \rho Q(t, x + \Delta x)v(t, x + \Delta x)] \\ &\approx -\rho \frac{\partial Q(t, x)v(t, x)}{\partial x} \Delta x \Delta t \end{aligned}$$

Accordingly, using $\rho = 1$, the equation of motion is written as

$$\frac{\partial Q}{\partial t} + \frac{\partial Qv}{\partial x} = F \quad (15)$$

where $F = F_{gravity} + F_{pressure} + F_{friction}$ is the sum of the external forces.

Gravitational force The total gravitational force F_g points down to the center of the earth and for the control volume it is given by

$$\begin{aligned} F_g &= -gm\hat{\mathbf{z}} \\ &= -g\rho A\Delta x\hat{\mathbf{z}} \end{aligned}$$

where $\hat{\mathbf{z}}$ denotes that the force is along the z axis. We only need the forces in the direction of flow for the equation of motion. Hence, we decompose F_g into two force components; namely, one in the direction of flow and one pointing down while being perpendicular to the direction of flow. The decomposition of the gravitational force is shown in Figure 7.

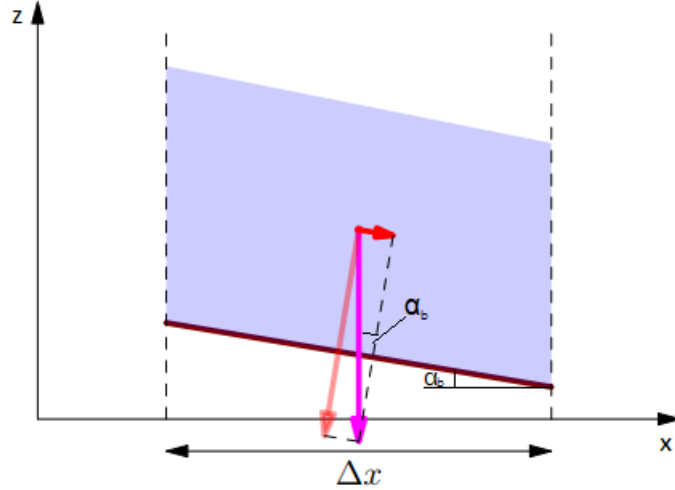


Figure 7: Decomposition of the gravitational force as illustrated in Figure 3.5 in [30]

Accordingly, by geometrical arguments using the angle α_b and the channel bed slope S_0 we derive the force in the flow direction, called F_0 for convenience

$$F_0 = \frac{\sin(\alpha_b)F_g}{\Delta x} = g\rho AS_0$$

where we use that for small α_b we have $S_0 = \tan(\alpha_b) \approx \sin(\alpha_b) \approx \alpha_b$ [30].

Pressure force Pressure force can generate flow momentum even if the channel bed slope is zero. We are assuming hydrostatic pressure, hence pressure increases linearly with depth. Thus, all pressure forces are generated by the differences in depths between the left and right of the control volume.

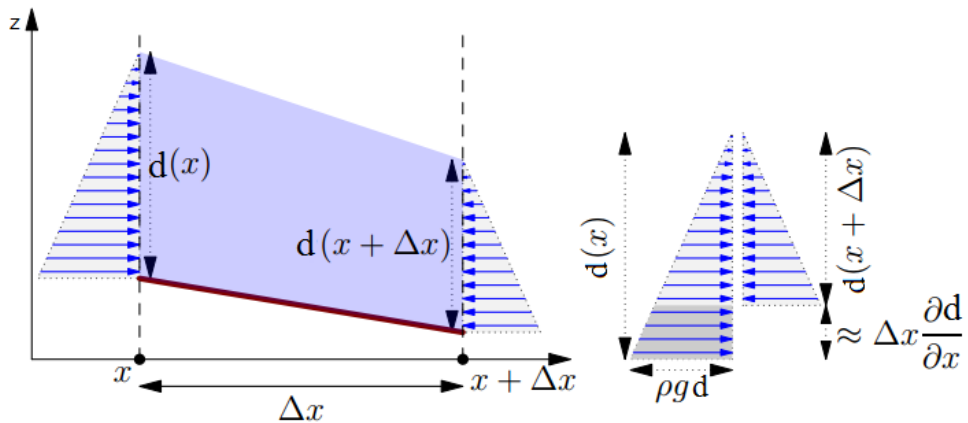


Figure 8: Graphical representation of the pressure forces on a control volume as illustrated in Figure 3.7 in [30]

As is shown in Figure 8, we have triangular pressure force fields due to hydrostatic pressure. Accordingly, we calculate the pressure force per unit length by evaluating the pressure differences between the cross sectional areas at x and $x + \Delta x$. Here, the y axis corresponds to the channel width.

$$\begin{aligned}
F_p &= \frac{\rho g}{\Delta x} \int dy \frac{d^2(x + \Delta x, y) - d^2(x, y)}{2} \\
&\approx \frac{\rho g}{-2\Delta x} \int dy \frac{\partial d^2(x, y)}{\partial x} \\
&= -\frac{\rho g}{2\Delta x} \int dy \Delta x \left[-2d(x, y) \frac{\partial d(x, y)}{\partial x} \right] \\
&= -\rho g \int dy \frac{\partial d(x)}{\partial x} \\
&= -\rho g \frac{\partial d(x)}{\partial x} A = -\rho g A S_p
\end{aligned}$$

where $\frac{\partial d(x)}{\partial x}$, the depth slope, is defined as the pressure slope S_p [30].

Friction force Flow loses momentum due to friction with the channel bed, plants, geographical structures, and so forth. Here, it is impossible to calculate the friction losses exactly because of the many different factors involved. Hence, the expressions for the friction force are highly empirical. Frictional forces created by the shear stress along the bottom and the sides of the control volume are given by $-\tau_0 P dx$ as derived by Chow [28], where τ_0 is the bed shear stress and P is the wetted perimeter. With $\tau_0 = \rho g \frac{A}{P} S_f$. Hence, similarly to the gravitational and the pressure forces, the friction force also takes the form

$$F_f = -\rho g A S_f$$

As was discussed in Section 3.2.5, S_f is the total energy gradient and can be determined empirically using Manning's Equation 12. Thus we get

$$S_f = \frac{n_m^2 Q}{A^2 R^{\frac{4}{3}}}$$

and accordingly the friction force becomes

$$F_f = \rho g A \frac{n_m^2 Q}{A^2 R^{\frac{4}{3}}}$$

To conclude, the equation of motion resulting from Equation (15) is

$$\frac{\partial Q}{\partial t} + \frac{\partial Qv}{\partial x} = gA(S_0 - S_f - S_p) \quad (16)$$

To summarise, the momentum equation consists of terms of physical processes governing the flow momentum. These terms are, from left to right in Equation (16) respectively, the *local acceleration* which is the change in momentum due to the change in velocity over time, the *convective acceleration term* which describes the change in momentum due to the change in velocity along the channel, the *gravity force term*, the *friction force term* and the *pressure force term* [28]. Note that the full equation of motion corresponds to unsteady, gradually varied (nonuniform) flow. Equation (16) can be simplified to the other, simpler types of flow by leaving out specific terms as is shown in Table 1.

$S_f = S_0$	steady uniform flow
$\frac{\partial Qv}{\partial x} = gA(S_0 - S_f - S_p)$	steady gradually varied flow
$\frac{\partial Q}{\partial t} = gA(S_0 - S_f)$	unsteady uniform flow
$\frac{\partial Q}{\partial t} + \frac{\partial Qv}{\partial x} = gA(S_0 - S_f - S_p)$	unsteady gradually varied flow

Table 1: Overview of the equation of motion for different types of flow

3.4 Geographical features

For this research we focus on a ditches network in North Friesland, called Polder Oude Bildtpollen. A map of the area is given in Figure 13, which can be found in the Appendix. The area contains a variety of geographical features such as waterway bifurcations, culverts, weirs, bridges, inlets and so forth. Here, we shall only consider the most important features since we are interested in the global water flow in the entirety of the ditches network. These are waterway bifurcations, weirs, pumping stations and culverts.

3.4.1 Waterway bifurcations and confluence conditions

The Polder Oude Bildtpollen waterway network has been digitalised and prepared for water flow modelling by Luc Scholten during his internship at Acacia

Water [25]. Here, a branch represents a length of a waterway. Branches are connected to each other by nodes. Hence, the network of branches and nodes represents the geographical data of the area to be modelled, given in Figure 13 in the Appendix. Each branch connects two nodes and has the following attributes:

- Begin node
- End node
- Branch length
- Information on the water flow; to be specified later, depending on which type of flow is modelled and which version of the Saint-Venant equations will be used

Each node can connect to multiple branches and waterway bifurcations can be modelled accordingly. The type of node is determined by the branches it connects to. One could express the network as a directed graph $G = (V, E)$, with V the set of nodes and E the set of directed edges which represent the direction of water flow. V_i is an inlet or outlet if for a $i \in 1, \dots, n$ with $n \in \mathbb{N}$, it connects to exactly one edge E_j where $j \in 1, \dots, m$ with $m \in \mathbb{N}$. A node is a connecting node of two smaller lengths of a waterway if it connects to exactly two edges E_j and E_k where $j \neq k$ and $j, k \in 1, \dots, m$. A node is a waterway bifurcation if it connects to three or more edges. See Figure 9 for an example of a waterway network.

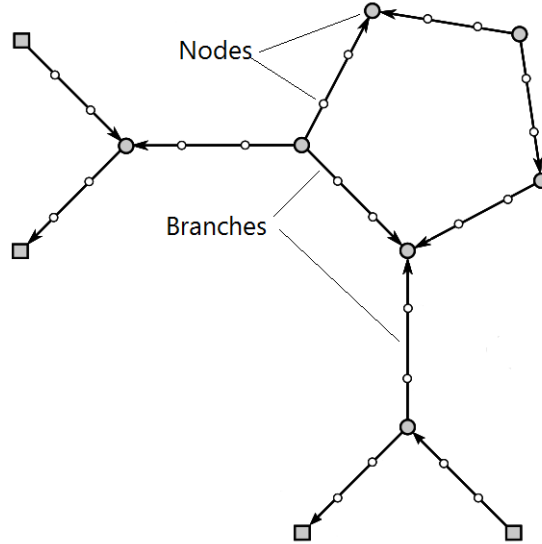


Figure 9: Network of nodes (grey and white circles and squares) and branches (black arrows), adapted from Figure 1.49 in [34]

Importantly, confluence conditions for the waterway bifurcations need to be specified. Specifically, waterway bifurcation nodes should satisfy the Saint-Venant equations for conservation of mass and conservation of momentum. To do so, a junction node is considered as a boundary node and discretized accordingly for each connected branch. Summing over the discretization of all the connected branches ensures two conservation laws to hold [34]. The precise mathematical derivation is a topic for research in the research project that follows from this literature review.

3.4.2 Weirs

Weirs are commonly used for measuring discharge in open channels. There are many different types of weirs which may be classified broadly into sharpcrested and broadcrested weirs. Which specific stage-discharge relationship to use is very dependent on the type of flow and the type of weir. Therefore, this is a point for further research at a later stage in the development of the water flow model.

3.4.3 Pumping stations, inlets or outlets

Water is removed from wetland areas by pumping stations, pumping excess fresh water into the sea. Data of the pumping stations can provide informa-

tion on discharge. Similarly, inlets or outlets are artificially controlled and can therefore provide information on the discharge. Therefore, both pumping stations, inlets and outlets can be considered as a given boundary condition for discharge in our model.

3.4.4 Culverts

A culvert is a construction which enables flow under a road or pathway. It imposes a unique kind of constriction on the open channel flow. A culvert may act as an open channel when its flow is partly full. It might seem like a simple hydraulic structure, however, it imposes complex flow conditions. These flow conditions are determined by many variables such as inlet geometry, size, roughness, slope and inlet and outlet conditions. Hence, determining flow through a culvert should be done empirically [27, 35]. In our research, we will take culverts into account by imposing a resistance on the flow through shrinking the cross sectional areas at the location of the culvert.

3.5 Salinity

In order to get an idea of the water salinity in the entire ditches network, we need to consider the salt concentrations (salt mass per unit volume) at every branch of the network. There are different ways of modelling these concentrations of varying complexity.

The most complicated method would be to incorporate the fluid density dependent variable ρ , considered as one of the unknown quantities, into the Saint Venant equations. In order to do so, the salt concentrations can be determined by the advection-diffusion equation, also called the transport equation, given by

$$\frac{\partial c}{\partial t} + v \frac{\partial c}{\partial x} + D \frac{\partial^2 c}{\partial x^2} = f \quad (17)$$

where c is the salt concentration, v the flow velocity, D the diffusion coefficient and f a source term. Subsequently, these salt concentrations are related to water densities in the Saint Venant equations [34]. In order to do so, we would need to consider the Navier Stokes equations from which we derive a new form

of the Saint Venant equations.

To simplify above method, one could consider the Saint Venant equations and the advection-diffusion equation separately. We will continue to assume the water density $\rho = 1$ in the Saint Venant equations and, at the same time, calculate the salt concentrations from Equation (18). This method will not be as accurate as above method because the densities will not be updated accordingly. However, it will give a rough idea on salinity.

The simplest method would be to apply a lumped approach for the salt mass balance. Similarly to the water storage equation, we would define a salt mass storage equation. Accordingly, we can apply the conservation of mass principle using a balance equation where the change in salt storage equals the sum of salt inflow and salt outflow.

A mathematical derivation and comparison between the possible methods will be further considered in the research project following from this literature review.

4 Mathematical problem formulation and solution methods

There are various methods available for applying either the simplified or the full Saint-Venant equations to modelling a water network. The main distinction between models is whether they apply the stationary or non-stationary Saint-Venant equations. Stationary models generally apply the continuity equation such as discussed for lumped routing, combined with either Manning's equation (10) for uniform flow or with the stationary Saint Venant equations combined with Manning's equation (12) for gradually varied flow [30,35]. Additionally, there is also the steady dynamic wave model which is equivalent to the stationary Saint Venant equations. Non-stationary models are classified as kinematic, diffusive or dynamic wave models which all use the full Continuity Equation (14) and variations of the Equation of Motion (16) [33]. In the following sections we discuss six models, of which three stationary and three non-stationary, applied to a ditches network of $n \in \mathbf{N}$ nodes. In all the models

we assume prismatic channels. Additionally, we assume depths and channel bed slopes to be known.

4.1 Flow conservation assuming equilibrium discharge

The simplest model is based on the continuity equation (1) for lumped flow routing and follows a pseudo-stationary approach. A channel is divided into reaches of very short equal lengths with each reach being represented by a control volume which has practically constant physical characteristics. Here, the physical characteristics are based on the equilibrium situation so the bed slope is assumed equal to the friction slope. Hence, the change in storage is calculated for each control volume at a given time t . Accordingly, water depths are updated and again calculated for subsequent times. Lateral inflow is not incorporated in the model equations. Instead, lateral flow is neglected if it is small compared to the in- and outflows or added or deducted from the inflow in case they are not negligible [28, 35].

To summarize the models main features and assumptions

- Lumped flow routing
- Pseudo-stationary approach; computes the flow rates and depths separately
- Uniform flow; equilibrium discharge
- Lateral flows incorporated in inflow, if not negligible
- Channel is divided into control volumes of equal lengths

System of equations Let us assume a simple channel of length L . We divide this channel into $n \in \mathbf{N}$ equal segments of length $\frac{L}{n}$, illustrating n control volumes which altogether form a river of water reservoirs. Accordingly, the change in storage is calculated for each control volume by the lumped flow routing Equation (1). Including lateral flow yields

$$\frac{dST}{dt} = Q_{in} - Q_{out} + Q_l \quad (18)$$

which in terms of discharge can be rewritten as

$$Q_{net} = Q_{in} - Q_{out} + Q_l \quad (19)$$

Considering segment $i \in N$, we can rewrite the storage equation into

$$\frac{dST_i}{dt} = Q_{i-1} - Q_i + Q_{l_i} \quad (20)$$

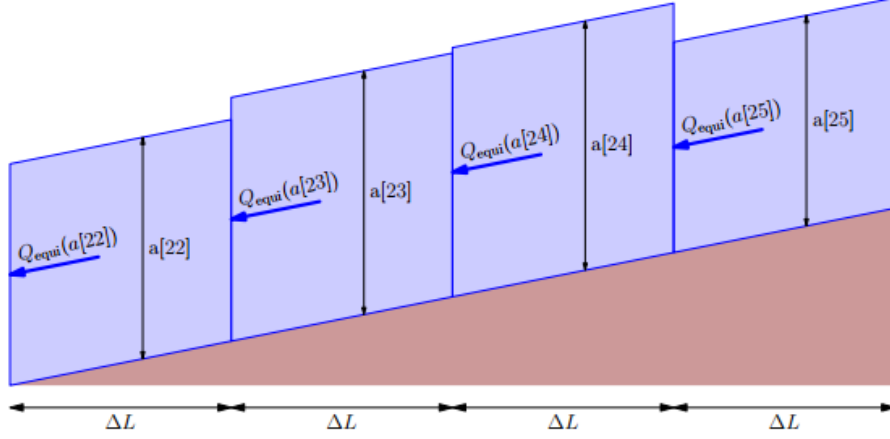
where the discharge is determined from the equilibrium discharge given by

$$Q_i = \frac{1}{n_m} S_0^{1/2} A_i R_i^{2/3}$$

assuming S_0 is a known constant along the channel. If S_0 is changing along the channel, one could also determine Q_i per control volume with, for instance,

$$Q_i = \frac{1}{n_m} \left(\frac{z_b(i+1) - z_b(i)}{\Delta x} \right)^{1/2} A_i R_i^{2/3}$$

The water level rises when $\frac{dST_i}{dt} > 0$ and falls when $\frac{dST_i}{dt} < 0$. Now consider a given time t_1 . We can calculate the $\frac{dST_i}{dt}$ for every cell of the channel and update the depths per cell by $S_i = S_i + \Delta S_i$, which is directly related to the depths in case of a rectangular channel with constant width; $d_i = d_i + \Delta d_i$. Consequently, we consider time t_2 and repeat the process. Hence, we arrive at a pseudo-stationary approach which means iterating a stationary system in time.



$$\frac{\partial S[24]}{\partial t} = Q_{\text{equi}}(a[25]) - Q_{\text{equi}}(a[24]) \quad S[24] = \Delta L A(a[24])$$

Figure 10: Graphical representation of lumped routing approach with the equilibrium discharge, taken from [30, 36]

Computational time and complexity In order to make a comparison in complexity and computational time among the six different models, we make the simplifying assumption of a broad rectangular channel for which holds that the wetted perimeter is approximately the width of the channel, i.e. $P \approx B$ so that $AR^{2/3} = Bd^{5/3}$. Accordingly, the stage-discharge relationship simplifies significantly. In this case we have, per timestep,

$$\begin{cases} \frac{dST_i}{dt} = Q_{i-1} - Q_i + Q_{l_i} & x_i \in (0, L) \\ Q_i = \frac{1}{n_m} B d_i^{5/3} S_0^{1/2} & x_i \in (0, L) \\ Q(x_0 = 0) = Q_0 \\ Q(x_n = L) = Q_N \end{cases} \quad (21)$$

Hence, at any timestep, we calculate the discharge Q_i for all segments except for the boundaries so for $i \in 1, \dots, n-1$. Subsequently, we calculate the change in storage $\frac{dST_i}{dt}$ for all segments $n \in \mathbb{N}$. Finally, the depths can be updated with $d_i = d_i + \Delta d_i$. Calculating the discharge requires taking a square root and one multiplication, assuming the $\frac{1}{n_m} B S_0^{1/2}$ to be a constant. Calculating the change in storage requires a subtraction and an addition. Updating the

water levels requires one more addition per control volume. Hence, assuming that the operations $+, -, *, /, \sqrt{}$ all have the same operational cost, for n_t timesteps we get a computational cost of

$$5n_x n_t$$

in order of flops needed for the calculations. n_x represents the number of spatial discretization steps; more spatial discretization steps results in more precise results. n_t represents the number of time steps chosen for which the stationary process is calculated.

4.2 Flow conservation with backwater effects

Here, again this model is based on the lumped routing continuity equation. Instead of calculating the discharge per control volume through the equilibrium stage-discharge equation, a new stage-discharge relation is determined from the full Saint Venant equations to incorporate the so called backwater effects; the effects of dams or obstructions in raising the water surface upstream from it. The general backwater equations are rewritten from the stationary Saint Venant equations as

$$\begin{cases} \frac{dQ}{dx} = Q_l \\ \frac{dd}{dx} = \frac{(S_0 - S_f - \frac{2vQ_l}{gA})}{1 - \mathbf{F}^2} \end{cases} \quad (22)$$

where \mathbf{F} is the Froude number which is defined in [30] by

$$\mathbf{F} = \sqrt{\frac{Q^2 b}{gA^3}} \quad (23)$$

Plugging in the equations for S_0 and S_f gives the following conservation of momentum equation

$$\frac{dd}{dx} = \frac{(\frac{\partial z_b}{\partial x} - \frac{n_m^2 Q |Q|}{R^{4/3} A^2} - \frac{2vQ_l}{gA})}{1 - \mathbf{F}^2} \quad (24)$$

Now, to derive a method for flow conservation with the backwater effects, we consider the following version of Saint Venant equations, with equilibrium

between gravity, friction and pressure, $S_0 - S_f - S_p = 0$ and no lateral inflow, which gives

$$\begin{cases} \frac{\partial Q}{\partial x} + \frac{\partial A}{\partial t} = 0 \\ \frac{\partial Q}{\partial t} + \frac{\partial Qv}{\partial x} = 0 \end{cases} \quad (25)$$

which results in the Jones' formula [37, 38]

$$Q = Q_{eq} \left(1 - \frac{1}{S_0} \frac{\partial d}{\partial x}\right)^{1/2} = \frac{1}{n_m} S_0^{1/2} AR^{2/3} \left(1 - \frac{1}{S_0} \frac{\partial d}{\partial x}\right)^{1/2} \quad (26)$$

Assuming that the Froude number $F = 0$, which is justified by considering that we're in a polder with slow water flow and small slopes, we arrive at

$$Q = \frac{1}{n_m} \left(\frac{\partial h}{\partial x}\right)^{1/2} AR^{2/3} \quad (27)$$

where $h = z_b + d$ is the water level, or stage, from datum to the water surface [30, 36].

To summarize the models main features and assumptions

- Lumped flow routing
- Pseudo-stationary approach; computes the flow rates and depths separately
- Nonuniform flow; incorporating backwater effects
- Stage-discharge relation derived by assuming $Q_l = 0$, $S_0 - S_f - S_p = 0$ and $F = 0$
- Lateral flows incorporated in inflow, if not negligible
- Channel is divided into control volumes of equal lengths

System of equations Similarly to the previous model, we have the storage function with a stage-discharge relationship. However, the stage-discharge relationship has now been derived from the backwater equations. The discretization is done a bit differently, since the bed channel slopes are assumed to be varying.

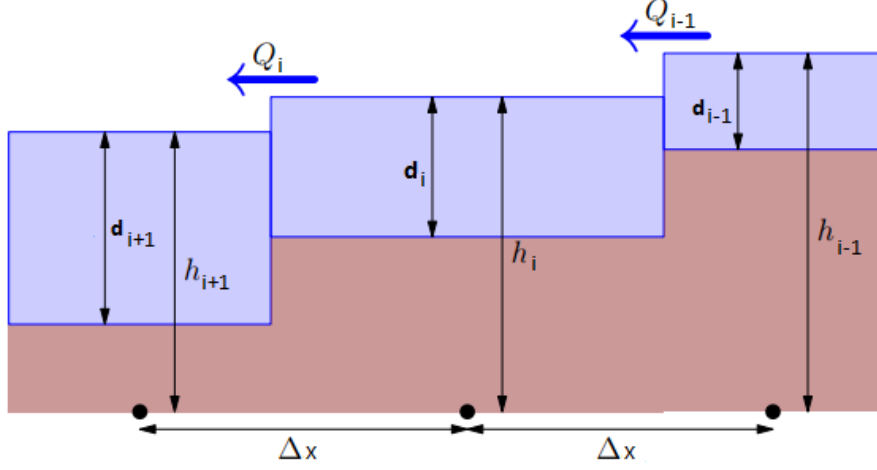


Figure 11: Graphical representation of lumped routing approach with the backwater discharge, taken and adapted from [30,36]

Accordingly, we arrive at the following system of equations, which differs slightly to the first model

$$\begin{cases} \frac{dST_i}{dt} = Q_i - Q_{i-1} + Q_{l_i} & x_i \in (0, L) \\ Q_i = \frac{B}{n_m} \left(\frac{d_{i+1} + d_i}{2} \right)^{5/3} \text{sign} \left(\frac{h_i - h_{i+1}}{\Delta x} \right) \left| \frac{h_i - h_{i+1}}{\Delta x} \right|^{1/2} & x_i \in (0, L) \\ Q(x_0 = 0) = Q_0 \\ Q(x_n = L) = Q_N \end{cases} \quad (28)$$

where the depths are subsequently updated according to $d_i = d_i + \Delta d_i$.

Computational time and complexity Here, the computational complexity of the discharge is larger than in the first model that we discussed. Now, it requires three additions, twice taking a root, once taking a sign, three times division and four multiplications. Hence, in total we arrive at a computational order of

$$16n_x n_t$$

4.3 Stationary Saint-Venant equations

The third stationary model follows directly from the full Saint-Venant equations. If we simply assume all time dependencies to vanish, we are left with

the stationary Saint-Venant equations

$$\begin{cases} \frac{dQ}{dx} = Q_l \\ \frac{dQv}{dx} = gA(S_0 - S_f - S_p) \end{cases} \quad (29)$$

Doing so leads to the backwater equations, in terms of the change in depths along the channel and the change in discharge along the channel which are usually written as

$$\begin{cases} \frac{dQ}{dx} = Q_l \\ \frac{dd}{dx} = \frac{S_0 - S_f}{1 - F^2} \end{cases} \quad (30)$$

These are generally used for studying the backwater effects on of weirs for example; which means that water is pushed back upstream due to a weir [26]. Commonly, the discharge is assumed to be known whereas the depths are assumed to be unknown. However, here we are interested in the discharge which is unknown. Accordingly, assuming the channel bed slope, initial depths and cross sectional areas are known, the discharges and updates depths can be calculated. In addition, we assume subcritical flow because of the mild slopes and slow water flow hence Froude's number $F < 1$.

To summarize the models main features and assumptions

- Steady flow; time derivatives are set to zero
- Nonuniform flow; incorporating backwater effects
- Pseudo-stationary approach; stationary situation is computed for fixed t and given water levels and cross sectional areas at that time, and subsequently updated with the new calculated values
- Subcritical flow due to mild slopes and slow flow velocities, thus $F < 1$
- Lateral flows are incorporated
- Depths, channel bed slopes and cross sectional areas are assumed to be known

System of equations In the stationary Saint Venant equations, we simply set all time dependencies to vanish. First we simplify the equation of motion

(30) as follows

$$\begin{aligned}
\frac{\partial Qv}{\partial x} &= gA(S_0 - S_f - S_p) \\
\Leftrightarrow \frac{1}{A} \frac{\partial Q^2}{\partial x} &= gA(S_0 - S_f - S_p) \\
\Leftrightarrow \frac{2Q}{A} \frac{\partial Q}{\partial x} - \frac{Q^2}{A^2} \frac{\partial A}{\partial x} &= gA \frac{\partial z_b}{\partial x} - \frac{gQ^2 n_m^2}{R^{4/3} A} - gA \frac{\partial d}{\partial x}
\end{aligned}$$

from which an example of a possible discretization can be given:

$$\left\{ \begin{array}{l} \frac{Q_i - Q_{i-1}}{\Delta x} = Q_{l_i} \quad x_i \in (0, L) \\ \frac{2Q_{l_i}}{A} Q_i + \left(\frac{gn_m^2}{R^{4/3} A} - \frac{1}{A^2} \left(\frac{A_i - A_{i-1}}{\Delta x} \right) \right) Q_i^2 = gA_i \left(\left(\frac{z_{b_i} - z_{b_{i-1}}}{\Delta x} \right) - \left(\frac{d_i - d_{i-1}}{\Delta x} \right) \right) \quad x_i \in (0, L) \\ Q(x_0 = 0) = Q_0 \\ Q(x_n = L) = Q_N \end{array} \right. \quad (31)$$

Additionally, when assuming a broad rectangular channel, the discretized second equation reads

$$\frac{2Q_{l_i}}{B} \frac{Q_i}{d_i} + \left(\frac{gn_m^2}{B^2 d_i^{10/3}} - \frac{1}{B d_i^2} \frac{d_i - d_{i-1}}{\Delta x} \right) Q_i^2 = gB d_i \left(\frac{z_{b_i} - z_{b_{i-1}}}{\Delta x} - \frac{d_i - d_{i-1}}{\Delta x} \right)$$

Hence, a detailed, but complicated expression to express dynamic waves. Ideally, one would rewrite the discretized equation with the unknown depths on the left hand side and all the other terms on the right hand side. Since this is a stationary equation, one updates the depths according to $d_i = d_i + \Delta d_i$.

Computational time This system of equations is considerably more complex than previous ones discussed, especially since the second equation yields a complex relation for calculating depths. For giving an indication on the computational time, we would need to further specify a method for solving this equation. Hence, this is an aspect for further research.

4.4 Kinematic wave model

The kinematic wave model is one possible simplifying model of the dynamic wave model. The dynamic wave model describes one dimensional unsteady,

gradually varied flow in open channels with Saint Venants equations and appropriate initial and boundary conditions [33]. For kinematic waves, the same assumptions hold as for dynamic waves, e.g. hydrostatic pressure and the friction slopes are based on Chézy's or Manning's equation. Additionally, the shallow water wave is assumed to be long and flat so that S_f almost equals the channel bed slope S_0 , hence secondary terms in equation of motion disappear. Thus, the bed slope, S_0 , is assumed to be large enough and the water wave long and flat enough so that the change in depth and velocity with respect to distance and the change in velocity with respect to time are negligible when subtracted from S_0 in the equation of motion. The discharge Q is assumed to be a function of the water depth alone, so there is only one wave speed in the direction along the channel. Hence, the wave celerity, or wave speed, is given by $c = \frac{\partial Q}{\partial A}$. Kinematic waves only propagate downstream and they do not attenuate as they propagate downstream [33].

To summarize the models main features and assumptions

- Distributed flow routing model; computes the flow rates and depths simultaneously
- It applies the full continuity equation and the equation of motion is replaced by the equation for uniform flow
- Shallow water waves are assumed to be long and flat, so that $S_0 \approx S_f$
- Discharge Q is a function of water depths alone
- Waves only propagate downstream and do not attenuate
- The wave celerity, or wave speed, is given by $c = \frac{\partial Q}{\partial A}$
- Lateral inflow can be incorporated in the continuity equation

System of equations The kinematic wave is defined as

$$\left\{ \begin{array}{l} \frac{\partial Q}{\partial x} + \frac{\partial A}{\partial t} = Q_l \quad x_i \in (0, L), t_j \in (0, t) \\ S_0 = S_f \quad x_i \in (0, L), t_j \in (0, t) \\ Q(x_0 = 0, t) = Q_0 \\ Q(x_n = L, t) = Q_N \end{array} \right. \quad (32)$$

which can be discretized using a finite difference approach as follows [28], again assuming a broad rectangular channel and S_0 given,

$$\left\{ \begin{array}{l} \frac{Q_{i+1}^{j+1} - Q_i^{j+1}}{\Delta x} + \frac{A_{i+1}^{j+1} - A_{i+1}^j}{\Delta t} = \frac{Q_{i+1}^{j+1} + Q_{i+1}^j}{2} \quad x_i \in (0, L), t_j \in (0, t) \\ Q_i^j = \frac{B}{n_m} S_0^{1/2} d_i^{5/3} \quad x_i \in (0, L), t_j \in (0, t) \\ Q(x_0 = 0) = Q_0 \\ Q(x_n = L) = Q_N \end{array} \right. \quad (33)$$

where $i \in (0, L)$ is the spatial discretization and $j \in (0, t)$ is the time discretization.

Computational complexity and time In the non-stationary approach, the depths and discharge values are calculated simultaneously. Hence, there is no separate depth update time step required. The continuity equation requires the following: For every discretization point in space i for $x_i \in (0, L)$ we require a subtraction and division. For every discretization point in time, an addition, a subtraction and two divisions are required. For calculating the discharge, one square root and one multiplication is required, assuming that $\frac{B}{n_m} S_0^{1/2}$ is a constant. Hence the computational complexity is of order

$$4n_x 4n_t = 16n_x n_t$$

4.5 Diffusive wave model

The diffusive wave model is another possible model simplifying the dynamic wave model. It is similar to the kinematic model, but incorporates the change

in water depths $\frac{\partial y}{\partial x}$. Diffusive waves also propagate downstream only at a celerity of $\frac{\partial Q}{\partial A}$. Unlike kinematic waves, diffusive waves attenuate as they propagate downstream [33]. Even though the diffusive wave does not include as many terms as the stationary Saint Venant equations, it appears to be more accurate. This is because the terms $\frac{\partial Q}{\partial t}$ and $\frac{\partial Qv}{\partial x}$ are usually of the same order of magnitude, but have opposite signs [33]. Thus, neglecting both of them is more accurate than including one of them.

To summarize the models main features and assumptions

- Distributed flow routing model; computes the flow rates and depths simultaneously
- It applies the full continuity equation and the equation of motion is simplified to an equation only incorporating S_0 , S_f and $\frac{\partial y}{\partial x}$
- Discharge Q is a function of water depths alone
- Waves only propagate downstream, but do attenuate as they move downstream
- The wave celerity, or wave speed, is given by $c = \frac{\partial Q}{\partial A}$
- Lateral inflow can be incorporated in the continuity equation

System of equations The system of equations for the diffusive wave model is given by

$$\left\{ \begin{array}{ll} \frac{\partial Q}{\partial x} + \frac{\partial A}{\partial t} = Q_l & x_i \in (0, L), t_j \in (0, t) \\ \frac{\partial d}{\partial x} = S_0 - S_f & x_i \in (0, L), t_j \in (0, t) \\ Q(x_0 = 0, t) = Q_0 \\ Q(x_n = L, t) = Q_N \end{array} \right. \quad (34)$$

which can be discretized using a similar approach as the kinematic wave equations, where the equation of motion is simplified in the same way as in (28) ,

as follows

$$\left\{ \begin{array}{l} \frac{Q_{i+1}^{j+1} - Q_i^{j+1}}{\Delta x} + \frac{A_{i+1}^{j+1} - A_i^j}{\Delta t} = \frac{Q_{i+1}^{j+1} + Q_i^j}{2} \quad x_i \in (0, L), t_j \in (0, t) \\ Q_i^j = \frac{B}{n_m} \left(\frac{h_{i+1}^{j+1} - h_i^{j+1}}{\Delta x} \right)^{1/2} d_i^{5/3} \quad x_i \in (0, L), t_j \in (0, t) \\ Q(x_0 = 0) = Q_0 \\ Q(x_n = L) = Q_N \end{array} \right. \quad (35)$$

where $i \in (0, L)$ is the spatial discretization and $j \in (0, t)$ is the time discretization.

Computational complexity and time Again, applying the same approach as to the kinematic wave equations, we arrive at a computational time of order

$$8n_x 4n_t = 24n_x n_t$$

.

4.6 Dynamic wave model

The dynamic wave refers to the distributed model applying the full Saint Venants equations. To be able to apply these, the assumptions for deriving the Saint Venants equations must hold, which are [28, 35]

1. The flow is one-dimensional, hence the axis along the channel is assumed to be a straight line. Depths and flow velocities are constant at any given cross section of a channel and only vary along the channel. Additionally, the water surface is horizontal across a cross section.
2. Flow rates are assumed to vary gradually along the channel so that hydrostatic pressure holds and vertical accelerations are negligible. This is true for mild slopes.
3. Chézy's and Manning's equations are applicable so that they can be used to describe the friction forces.
4. The water is of constant density

Accordingly, dynamic waves propagate both upstream and downstream and they do attenuate. Therefore, in this model both upstream and downstream boundary conditions need to be specified. General guidelines on when to apply which model have been specified, but it depends on the situation whether these are applicable [33].

Solution methods The solution methods available for solving the the full Saint-Venant equations for unsteady flow are, discussed in for example [26–28, 31, 35],

1. The method of characteristics
2. Finite difference method
3. Finite volume method
4. Finite element method

where also a combination of methods can be used, see for example [40].

5 Conclusion

For the Spaarwater project we are looking for a simple and fast method to model the water flow in the ditches network. The final goal is to use this method for a fast mobile phone application. Commonly, the one dimensional Saint Venant equations are used for modelling this type of open channel flow either through a lumped or distributed modelling approach. In this literature review, we have discussed both methods. In total, we have examined six different possible versions of the Saint Venant equations. However, note that this is not an exhaustive list of all possible versions of the Saint Venant equations.

In a lumped model, the continuity equation is expressed in terms of the change in storage per channel segment. Accordingly, the conservation of momentum equation can be simplified in different ways to find a relation for the discharge which is necessary for solving the continuity equation. For this approach the water depths and channel bed slopes are assumed to be known. Hence, the change in storage is calculated at a fixed time and updated per timestep accordingly.

On the other hand, in a distributed model, a system of partial differential equations is solved. In this literature review, we have discussed four possible systems of equations for distributed modelling derived from the full one dimensional Saint Venant equations; namely, the stationary Saint Venant equations, the kinematic wave equation, the diffusive wave equation and the full Saint Venant equations, also referred to as the dynamic wave equation.

The stationary Saint Venant equations describe detailed wave motion in a fixed moment in time. It could serve as a good starting point for modelling instationary wave motion through a pseudo-stationary approach. How to implement this pseudo-stationary approach is a point for further research, especially since the continuity equation has been simplified such that it does not represent the conservation of flow. Important to note is that this would model wave motion on small scales with much detail. Therefore, this might not be the most preferable options. One of the instationary models could be better for giving a fast and general idea of the waterflow.

The kinematic, diffusive and dynamic wave equations automatically incorporate the timesteps in their computations. These models vary in their level of detail depending on which version of the conservation of momentum equation is applied. The kinematic wave simply models uniform waves with large wavelengths. The diffusive wave models nonuniform waves incorporating backwater effects, thus modelling attenuating waves. The full Saint Venant equations model waves on local scales which move both upstream and downstream and which also attenuate.

The computational times are slightly smaller for the lumped approach when we compare the uniform flow situations for the lumped (with Q_{eq}) and the distributed (kinematic wave) approach; namely, the computational times are of order $5n_x n_t$ and $16n_x n_t$ respectively. We do not expect this to be a significant difference in the scale of the ditches network under consideration. The advantage of a lumped approach is its simplicity and speed. A distributed approach yields a more detailed and flexible model in which both variation in space and time are calculated simultaneously without adding significant increase in computational costs. It will be a more flexible method for calculating water flow in larger networks.

6 Project proposal

There are many possible research directions varying in complexity. Therefore, it is important to define the scope of the research project. We discussed six different models in this literature review which we could all possibly implement. However, implementing each one of them is beyond the scope of this research. Therefore, we will choose one model to start with. Accordingly, we will investigate this model's implementation and performance. Based on the results, we either build further on this model or investigate another model for comparison. Important is to start simple and increase model complexity on the way.

We propose to start with implementing the simplest distributed model; namely, the kinematic wave equations. It allows for both the discharge and

the water depths to be unknown, which resembles the real situation. It means that we will consider an instationary model. However, when only considering one timestep, the distributed model resembles the lumped model/pseudo-stationary approach.

6.1 Project goal and research questions

The aim of the project is to make a first small step in modelling the water-flow in a ditches network. The main focus is developing the mathematical implementation and thereby a further understanding of the models discussed in this literature review. In doing so, we aim to answer the following research questions:

1. How do we discretize the kinematic wave equations using the finite volume method?
2. How does the kinematic wave equation compare to the other possible models in terms of its applicability, computational time and accuracy?
3. How do we design the grid such that it represents the geographical structure of a ditches network?
4. How do we decide on the boundary conditions and how do we implement boundary and confluence conditions into the grid, incorporating different flow directions?

6.2 Methods

The model will have to be designed such that it fits into Acacia Water's software infrastructure. Therefore, Python 3 will be the programming language. We will consider different model problems of increasing difficulty in order to answer abovementioned research questions.

Straight ditch The simplest test model is a straight ditch of length L with $n \in \mathbf{N}$ nodes and branches of length $\frac{L}{n-1}$. We will need to incorporate suitable boundary conditions. We can extend this simple model by adding a culvert, dam or pumping station to the ditch.

Network with two waterway bifurcations The next test model has $n \in \mathbf{N}$ nodes of which two nodes have three neighbouring branches, thus including two waterway bifurcations. We will have to apply both boundary conditions and confluence conditions to this problem.



Figure 12: Test problem with two waterway bifurcations

Network with multiple waterway bifurcations The last test model will be to apply the developed model to part of a real case ditches network. If and how much we can do for this test problem depends on the progress on the modelling of the previous two test problems.

References

- [1] UNESCO World Heritage Centre, “UNESCO World Heritage Centre - Decision - 33 COM 8B.4.” [Online]. Available: <http://whc.unesco.org/en/decisions/1946>
- [2] D. Waddenacademie, “Social and spatial economics.” [Online]. Available: <https://www.waddenacademie.nl/en/themes/social-and-spatial-economics/>
- [3] Common Wadden Sea Secretariat (CWSS) and Working Group on Landscape and Cultural Heritage (WADCULT), “THE WADDEN SEA REGION A Living Historic Landscape,” 2007. [Online]. Available: http://www.waddensea-secretariat.org/sites/default/files/downloads/lwp_strategy_brochure.pdf
- [4] L. Tolk and J. Velstra, “Spaarwater, pilots rendabel en duurzaam agrarisch watergebruik in een verziltende omgeving van de waddenregio,” Acacia Institute, Tech. Rep., 2016. [Online]. Available: http://www.spaarwater.com/content/27227/download/clnt/67009_Spaarwater_hoofdrapport_2016.pdf
- [5] LTO Noord, “Noord-Holland.” [Online]. Available: <https://www.ltonoord.nl/provincie/regio-west/noord-holland>
- [6] —, “Flevoland.” [Online]. Available: <https://www.ltonoord.nl/provincie/regio-west/flevoland>
- [7] —, “Groningen.” [Online]. Available: <https://www.ltonoord.nl/provincie/regio-noord/groningen>
- [8] A. M. van Dam, O. A. Clevering, W. Voogt, T. G. L. Aendekerk, and M. P. van der Maas, “Leven met Zout Water,” Praktijkonderzoek Plant & Omgeving B.V., Tech. Rep., 2007. [Online]. Available: http://www.stowa.nl/Upload/nieuws/LevenmetZoutWater_DeelrapportZouttolerantieLandbouwgewassen.pdf

- [9] H. de Boer and S. Radersma, “Verzilting in Nederland: oorzaken en perspectieven,” Wageningen UR Livestock Reserach, Tech. Rep. November, 2011. [Online]. Available: <http://library.wur.nl/WebQuery/groenekennis/1975852>
- [10] A. Subramani, M. Badruzzaman, J. Oppenheimer, and J. G. Jacangelo, “Energy minimization strategies and renewable energy utilization for desalination: A review,” pp. 1907–1920, feb 2011. [Online]. Available: <https://www.sciencedirect.com/science/article/pii/S0043135411000042>
- [11] R. G. Raluy, L. Serra, and J. Uche, “Life cycle assessment of desalination technologies integrated with renewable energies,” *Desalination*, vol. 183, no. 1-3, pp. 81–93, nov 2005. [Online]. Available: <http://www.sciencedirect.com/science/article/pii/S001191640500490X?via%3Dihub>
- [12] G. Van Staveren and J. Velstra, “Verzilting van landbouwgronden in Noord-Nederland in het perspectief van de effecten van klimaatsverandering,” Acacia Institute, Tech. Rep., 2012. [Online]. Available: <http://www.acaciadata.com/doc/Syntheserapport-278-VerziltingvanlandbouwgrondeninNoordNederland.pdf>
- [13] A. de Vos, J. Rozema, M. van Rijsselberghe, W. van Duin, and W. Brandenburg, “Zilte Landbouw Texel,” Vrije Universiteit Amsterdam; Texelse Milieuvriendelijke Natuurprodukten B.V.; Imares Wageningen UR; Wageningen UR, Tech. Rep., 2010.
- [14] A. de Vos, B. Bruning, G. van Straten, R. Oosterbaan, J. Rozema, and P. van Bodegom, “Crop salt tolerance under controlled field conditions in The Netherlands, based on trials by Salt Farm Texel,” Salt Farm Texel, Tech. Rep., 2016. [Online]. Available: http://www.saltfarmtexel.com/application/files/2215/0125/0486/Final_report_Crop_Salt_Tolerance-Salt_Farm_Texel.pdf
- [15] E. van Essen, B. Snellen, J. Kroes, and L. Stuyt, “Sociaal-economisch spoor verzilting Noord-Nederland,” Acacia Institute, Tech. Rep., 2011.

- [Online]. Available: <http://www.acaciadata.com/doc/Eindrapport-278-Sociaal-EconomischspoorverziltingNoord-Nederland.pdf>
- [16] J. Velstra and A. de Vries, “Nieuwe kijk op verzilting biedt perspectief voor zoetwatertekort,” *H2O*, vol. 22, pp. 20–21, 2008. [Online]. Available: <http://edepot.wur.nl/67518>
- [17] J. Fiselier, E. Benner, A. van de Kerk, M. de Haan, R. de Koning, L. Bos, and R. Hoekstra, “Zilte Perspectieven,” DHV, Amersfoort; CLM, Utrecht, Tech. Rep., 2003. [Online]. Available: <http://edepot.wur.nl/118130>
- [18] P. de Louw, “Saline seepage in deltaic areas: Preferential groundwater discharge through boils and interactions between thin rainwater lenses and upward saline seepage,” Ph.D. dissertation, 2013. [Online]. Available: <https://research.vu.nl/ws/portalfiles/portal/964702>
- [19] J. R. Delsman, “Saline groundwater – Surface water interaction in coastal lowlands,” Ph.D. dissertation, VU University, 2015.
- [20] G. O. Essink, “Effect zeespiegelstijging op het grondwatersysteem in het kustgebied,” *H2O*, no. 19, pp. 60–64, 2007. [Online]. Available: <http://edepot.wur.nl/343127>
- [21] S. Barten, K. van Diepen, L. Frölke, and J. Pouwels, “Klimaatverandering in de polder,” Acacia Institute, Tech. Rep., 2017.
- [22] P. Schipper, A. Veldhuizen, and J. Kroes, “Effectief inlaatregiem zoetwatervoorziening Pilot modellering Eureyeopener voor het Hoogheemraadschap Hollands Noorderkwartier,” Alterra, Wageningen, Tech. Rep., 2016. [Online]. Available: <http://edepot.wur.nl/400551>
- [23] J. de Wit, “How effective is the process of fresh inlet water in a polder area subjected to saline seepage? The effect of fresh inlet water on salinity of surface water bodies in a closed wetland system,” Ph.D. dissertation, VU University, 2016.

- [24] S. Hendriks, “How effective does the inlet water, supplied to a low lying polder region, freshen the ditches network ?” Ph.D. dissertation, VU University, 2016.
- [25] L. Scholten, “Ruimtelijke verdeling van water in de polder; Automatisering van een distributie oppervlakte water model,” Tech. Rep., 2017.
- [26] T. W. Sturm, *Open channel hydraulics*. Boston: McGraw-Hill, 2010. [Online]. Available: <https://tudelft.on.worldcat.org/search?queryString=no:840409841&databaseList=4096,4058,2375,3441,2572,1953,1875,3535,1697,3413,3313,638,3954,2264,3551,3450,2261,2062,2260,3404,2237,2259,2897,2038,2059,3544,3988#/oclc/840409841>
- [27] M. H. Chaudhry, *Open-Channel Flow*. Boston, MA: Springer US, 2008. [Online]. Available: <http://link.springer.com/10.1007/978-0-387-68648-6>
- [28] V. T. Chow, D. R. Maidment, and L. W. Mays, *Applied Hydrology*, mcgraw-hil ed. New York: McGraw-Hill, 1988.
- [29] L.-C. Lundin, S. Bergström, E. Eriksson, and J. Seibert, “Hydrological models and modelling,” pp. 129–140, 1998.
- [30] P. J. J. F. Torfs, *Open channel flow [Course notes]*. Wageningen (the Netherlands): Hydrology and Quantitive Water Management Group, 2013.
- [31] J. F. Cruise, M. M. M. M. Sherif, and V. P. V. P. Singh, *Elementary hydraulics*. Toronto: Thomson/Nelson, 2007.
- [32] E. P. Querner, “Aquatic weed control within an integrated water management framework,” DLO Winand Staring Centre, Wageningen (the Netherlands), Tech. Rep., 1993. [Online]. Available: <http://www.querter.eu/site/Ned-onderzoek/Report-67-PhD-Querner-juni1993.pdf>
- [33] J. E. Miller, “Basic Concepts of Kinematic-Wave Models,” *U.S. Geol. Surv. Prof. Pap. 1302*, 1983. [Online]. Available: <https://pubs.usgs.gov/pp/1302/report.pdf>

- [34] Deltares, “D-Flow 1D (SOBEK 3); technical reference manual,” Delft, 2017. [Online]. Available: http://content.oss.deltares.nl/delft3d/manuals/D-Flow1D_Technical_Reference_Manual.pdf
- [35] V. T. Chow, “Open-channel hydraulics,” *McGraw-Hill B. Co.*, p. 728, 1959.
- [36] P. J. J. F. Torfs, *Hydraulics and Hydrometry [Course notes HWM-21806]*. Wageningen (the Netherlands): Hydrology and Quantitative Water Management Group, 2017.
- [37] H. Hidayat, B. Vermeulen, M. G. Sassi, P. J. J. F. Torfs, and A. J. F. Hoitink, “Discharge estimation in a backwater affected meandering river,” *Hydrol. Earth Syst. Sci.*, vol. 15, pp. 2717–2728, 2011. [Online]. Available: www.hydrol-earth-syst-sci.net/15/2717/2011/
- [38] A. Petersen-Overleir, “Modelling stage-discharge relationships affected by hysteresis using the Jones formula and nonlinear regression,” *Hydrol. Sci. J.*, vol. 51, no. 3, pp. 365–388, 2006.
- [39] G. W. Brunner, “HEC-RAS, River Analysis System Hydraulic Reference Manual,” US Army Corps of Engineers; Hydrologic Engineering Center, Tech. Rep., 2016. [Online]. Available: <http://www.hec.usace.army.mil/software/hec-ras/documentation/HEC-RAS5.0ReferenceManual.pdf>
- [40] K. Unami and A. H. M. B. Alam, “Concurrent use of finite element and finite volume methods for shallow water flows in locally 1-D channel networks,” *Int. J. Numer. Methods Fluids*, vol. 69, no. 2, pp. 255–272, may 2012. [Online]. Available: <http://doi.wiley.com/10.1002/flid.2554>
- [41] Werkgroep Herziening Cultuurtechnisch vademecum, *Cultuur technisch vademecum; deel III water*, 1988.
- [42] Wetterskip Fryslân, “Watersysteem: Polder Oude Bildtpollen en Noorderleegpolder,” Leeuwarden, 2015.

A Geographical information

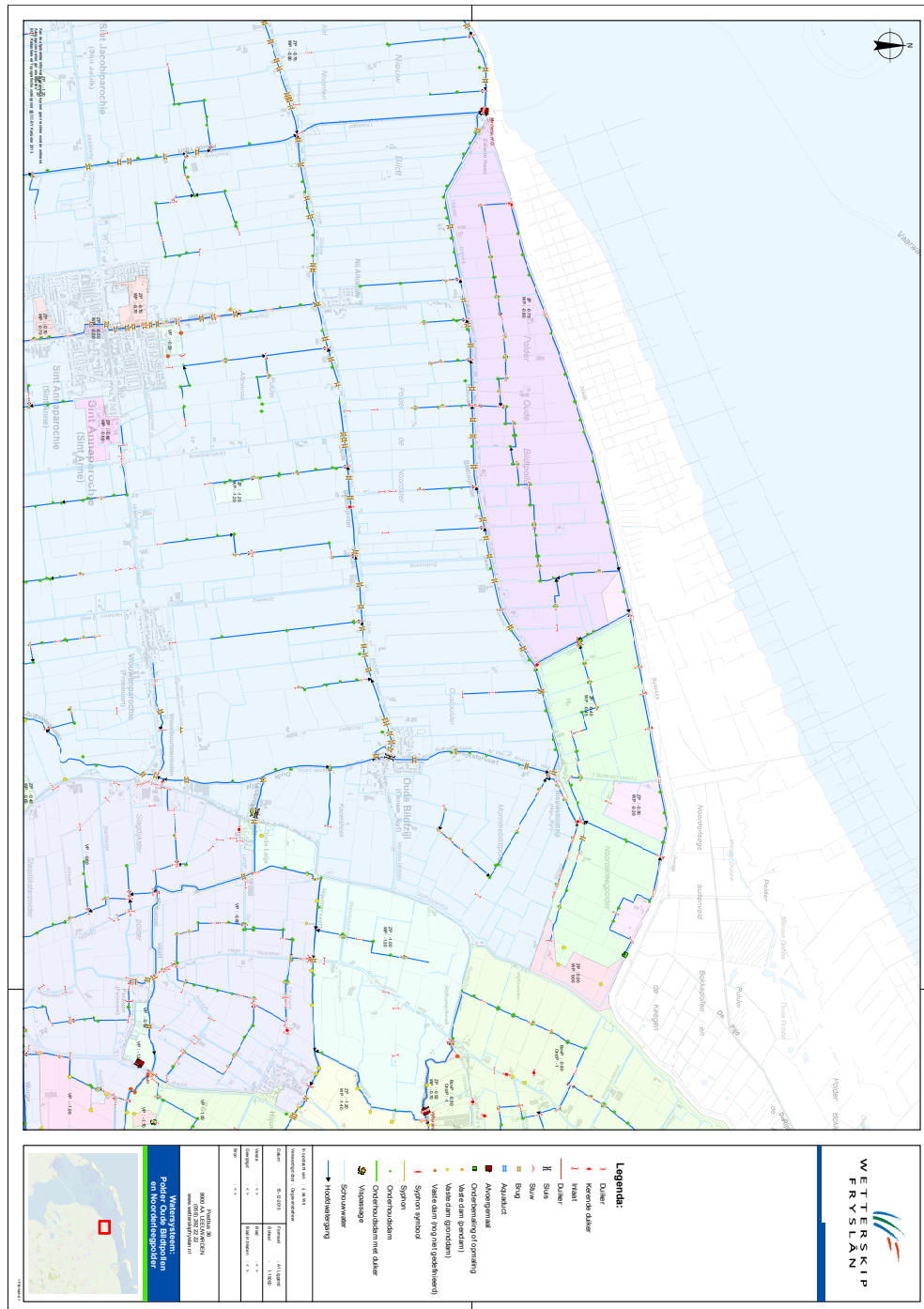


Figure 13: Map of the ditches network in which the Polder Oude Bildtpollen is shown in purple on the left of the map. Source: Wetterskip Fryslân [42].